Circular RNA-MTO1 suppresses breast cancer cell viability and reverses monastrol resistance through regulating the TRAF4/Eg5 axis

YUNXIAO LIU, YANYAN DONG, LIPING ZHAO, LIHONG SU and JIN LUO

Department of Pathology, Shanxi Province People's Hospital, Taiyuan, Shanxi 030001, P. R. China

Received January 23, 2018; Accepted May 24, 2018

DOI: 10.3892/ijo.2018.4485

Abstract. Circular RNAs (circRNAs), a class of endogenous RNAs, have emerged as an enigmatic class of genes. However, little is known about their value in the progression and chemoresistance of cancers. The present study sought to determine the expression profiles and potential modulatory role of circRNAs on breast cancer cell viability and monastrol resistance. Monastrol-resistant cell lines were established by exposing breast cancer cells to increasing concentrations of monastrol. A human circRNA microarray was used to search for dysregulated circRNAs in monastrol-resistant cells, then circRNA-MTO1 (hsa-circRNA-007874) was validated as a circRNA that exhibited elevated expression levels in monastrol-resistant cells. Mechanistic investigations suggested that upregulation of circRNA-MTO1 suppressed cell viability, promoted monastrol-induced cell cytotoxicity and reversed monastrol resistance. Subsequently, Eg5 was identified as the functional target of circRNA-MTO1, and MTO1 inhibited Eg5 protein level but not mRNA level. By treating with protein synthesis inhibitor cycloheximide (CHX), it was revealed that MTO1 did not affect the protein stability of Eg5. RNA-pull down experiments followed by mass spectrometry revealed that MTO1 interacted with tumor necrosis factor receptor associated factor 4 (TRAF4), and sequester TRAF4 from activating Eg5 translation, thereby inhibiting the Eg5 protein level. Taken together, the data reveal a regulatory mechanism by circRNA-MTO1 to control cell viability and monastrol resistance in breast cancer cells.

Introduction

Breast cancer is one of the leading causes of cancer-associated mortalities worldwide and the most common cancer among women (1). The majority of patients are at advanced stages at the time of diagnosis, and the prognosis of these patients remains poor (2). Currently, adjuvant chemotherapy and radiotherapy following surgical resection is the most commonly used treatment strategy, however, the 5-year survival rate of breast cancer remains low, and the improvement of prognosis of breast cancer patients has reached a plateau (3,4). Therefore, finding promising therapeutic and prognostic targets is essential for developing effective therapies for breast cancer patients.

Drugs that target the mitotic spindle are among the most effective cancer therapeutics currently in use. In addition, there is hope that such drugs would not produce debilitating neuropathies such as those caused by treatment of cancer with taxanes (5). Monastrol, the prototype anti-kinesin drug, is known to inhibit the mitotic motor Eg5 (6-8), which is a member of a family of kinesins crucial for maintaining separation of the half-spindles (9,10). Treatment of dividing cells with monastrol results in the collapse of the bipolar spindle into a non-functional monastral spindle. However, the underlying functional mechanism and interaction between Eg5 and monastrol is not well known.

High-throughput RNA sequencing (RNA-Seq), an emerging method to study the RNA regulation mechanism in the whole genome, has been able to detect circular RNA (circRNAs) (11). Circular RNAs (circRNAs) are a large class of endogenous RNAs that are formed by exon skipping or back-splicing events with neither 5' to 3' polarity nor a polyadenylated tail; however, they attracted little attention until their function in post-transcriptional regulation of gene expression was discovered. circRNAs are conserved and stable, and numerous circRNAs seem to be specifically expressed in a cell type or developmental stage (12,13). The cell type- or developmental stage-specific expression patterns indicate that circRNAs may be important regulators in various diseases, including heart cerebrovascular disease, hematological disease and malignant tumors (14).

circRNAs participate in several different biological processes in cancer cells, including cell growth, metastasis, cell cycle control, nuclear and cytoplasmic trafficking, cell differentiation, RNA decay, transcription and translation (15). In the cytoplasm, circRNAs may function as competing endogenous RNAs (ceRNAs), thus inducing the suppression of genes that are targeted by specific miRNAs (16). Previously, it has been reported that they can act as scaffolds to directly

Correspondence to: Dr Yunxiao Liu, Department of Pathology, Shanxi Province People's Hospital, 29 Twin Towers Temple Street, Taiyuan, Shanxi 030001, P.R. China
E-mail: sxlyx7402@126.com

Key words: circular RNA-MTO1, breast cancer, Eg5, tumor necrosis factor receptor associated factor 4, monastrol

bind to specific proteins and to hire gene-modifying bodies to silence or activate targeted genes (17). To date, verifying the deregulated circRNAs and further investigating the underlying regulatory mechanism in breast cancer cells is still an ongoing process.

The present study investigated monastrol-induced circRNA regulation in breast cancer by performing a genome-wide microarray in cells that were treated with monastrol. In addition, it was identified that, circRNA MTO1 (hsa-circRNA-007874), inhibits Eg5-mediated cell viability and promotes chemosensitivity through sequestering TRAF4 from binding to Eg5 protein.

Materials and methods

Cell culture and reagents. The human breast cancer cell lines MDA-MB-231, MCF-7, MDA-MB-453, SKBR-3, T47D and MDA-MB-468 were purchased from Chinese Academy of Sciences (Shanghai, China). All breast cancer cell lines were cultured with high glucose-Dulbecco's modified Eagle's medium (DMEM) supplemented with 10% fetal bovine serum (FBS; Gibco; Thermo Fisher Scientific, Inc., Waltham, MA, USA) at 37˚C in a humidified incubator with 5% CO_2. Cycloheximide (CHX) was purchased from Sigma-Aldrich (Merck KGaA, Darmstadt, Germany) and used for treatment of breast cancer cells for 80 min followed by western blot analysis to determine Eg5 protein level.

Development of monastrol-resistant breast cancer cell lines. MCF-7-R and MDA-MB-231R cell lines were developed by exposing parental MCF-7 and MDA-MB-231 parental cells to an initial dose of 10 μM monastrol (Sigma-Aldrich; Merck KGaA) in DMEM supplemented with 10% FBS for 6 weeks. Cells were cultured for three passages to reach a confluence of 70%. The survival cells were then cultured in 20 μM monastrol for 8 weeks and 50 μM monastrol for a further 8 weeks to obtain the resistant population. The monastrol-resistant cell lines were eventually established by culturing the cells in monastrol at a concentration of 100 μM. During the experiments, both monastrol-resistant cell lines were cultured to no higher than 10 passages.

Expression profile analysis of circRNAs. Total RNAs were extracted from breast cancer cells and quantified using the NanoDrop ND-2000 (Nanodrop Technologies; Thermo Fisher Scientific, Inc., Wilmington, DE, USA). circRNA expression analysis was performed according to the Arraystar protocol (18). Following hybridization and washing of samples, six breast cancer cell lines (MCF-7, MDA-MB-231, MDA-MB-468, MDA-MB-453, SKBR-3 and T47D) and two monastrol resistant cell lines (MCF-7R and MDA-MB-231R) were amplified and labeled using the RNeasy Mini kit (Qiagen GmbH, Hilden, Germany). A hybridization solution was then prepared and added to the circRNA expression microarray slide and incubated at 65˚C for 16 h. Subsequently, the slides were scanned by the Axon GenePix 4000B microarray scanner and imported into GenePix Pro 6.0 software (Molecular Devices, LLC, Sunnyvale, CA, USA). The microarray analysis was conducted by Beijing Genomics Institute/HuaDa-Shenzhen (Shenzhen, China).

RNA oligoribonucleotides and cell transfection. The circRNA-MTO1 overexpression plasmid was synthesized by Shanghai GenePharma Co., Ltd (Shanghai, China) and an empty vector used as a control. The Eg5 overexpression vector was purchased from OriGene Technologies, Inc. (Rockville, MD, USA) and an empty vector used as a control. The breast cancer cells were plated at $5x10^4$ cells/well in 24-well plates approximately 24 h prior to transfection. After the cells reached 30-50% confluence, transfection was carried out using Lipofectamine® 3000 (Invitrogen; Thermo Fisher Scientific, Inc., Waltham, MA, USA) following the manufacturer's protocol. The final concentration of circRNA-MTO1 overexpression plasmid, Eg5 overexpression vector, and the respective empty control vectors were 100 nM. Transfection efficiency was evaluated by labeling vectors with green fluorescence protein (GFP) to ensure that cells were successfully transfected. Functional experiments were then performed 48 h following sufficient transfection.

Cell viability assay. The altered cell viability following transfection or other treatments was assayed using a Cell Counting Kit (CCK)-8 assay (Dojindo Molecular Technologies, Inc., Kumamoto, Japan). In brief, breast cancer cell lines were seeded into a 96-well plate in triplicate and then treated with circ-MTO1 and (or) Eg5 overexpression vector for different time periods. Following this, cell cultures were treated with the CCK8 reagent (10 ml) and further cultured for 2 h. The optical density at a wavelength of 450 nm was measured with a spectrophotometer (Thermo Electron Corporation, Waltham, MA, USA). The percentage of the control samples of each cell line was calculated thereafter.

Nuclear fractionation. Nuclear fractionation was performed with a PARIS™ Kit (Ambion; Thermo Fisher Scientific, Inc.). For nuclear fractionation, $1x10^7$ cells were collected and resuspended in the cell fraction buffer and incubated on ice for 10 min. Following centrifugation (4˚C and 500 x g for 3 min), the supernatant and nuclear pellet were preserved for RNA extraction using a cell disruption buffer according to the manufacturer's protocol.

Reverse transcription-quantitative polymerase chain reaction (RT-qPCR). Total RNA was isolated from breast cancer cells using TRIzol® reagent (Invitrogen; Thermo Fisher Scientific, Inc.,). RT-qPCR of individual RNAs was performed by using a TaqMan RNA Reverse Transcription Kit (Applied Biosystems; Thermo Fisher Scientific, Inc.) and TaqMan Human RNA Assay kit (Applied Biosystems; Thermo Fisher Scientific, Inc.). The thermocycling conditions were 95˚C for 10 min, followed by 40 cycles of 95˚C for 15 sec and 60˚C for 1 min. The comparative cycle threshold (Cq) method was used to calculate the relative abundance of RNA compared with GAPDH expression (19). The primer sequences used were as follows: Forward, 5'-GGGTGTTTACGTAGACCAGA ACC-3', reverse, 5'-CTTCCAAAAGCCTTCTGCCTTAG-3' for circRNA-MTO1; forward, 5'-GAACAATCATTAGCAGC AGAATRAF4-3', reverse, 5'-TCAGTATAGACACCACAG TTG-3' for Eg5 and forward, 5'-GCACCGTCAAGGCTGAG AAC-3', reverse, 5'-ATGGTGGTGAAGACGCCAGT-3' for GAPDH. Each experiment was performed in triplicate.

circRNAs immunoprecipitation (circRIP). Biotin-labeled circRNA-MTO1 probe (5'-AAAGGAAGGATTACATGACA TCTGACCCAAAA CAACCCCACTGACA-3'-biotin) was synthesized by Sangon Biotech Co., Ltd. (Shanghai, China) and the circRIP assay was performed as previously described with minor modifications (20). circRIP was conducted by using MCF-7 and MCF-7R cells with Magna RIP™ RNA-binding protein immunoprecipitation kit (EMD Millipore, Billerica, MA, USA) according to the manufacturer's protocol. A total of $1x10^7$ cells were lysed in complete RNA lysis buffer, then cell lysates were incubated with RIP immunoprecipitation buffer containing magnetic beads conjugated with human anti-TRAF4 antibody (EMD Millipore, cat. no. #MABC985) or negative control IgG (EMD Millipore, cat. no. #PP64). Samples were incubated with Proteinase K and then immunoprecipitated RNA was isolated. Extracted RNAs were analyzed by RT-qPCR to identify the interaction.

RNA pulldown and mass spectrometry. Cells were lysed and incubated with biotin-labeled MTO1 (Sangon Biotech Co., Ltd.,) overnight. The proteins associated with biotin-labeled RNA were then pulled down with Streptavidin Magnetic Beads (Thermo Fisher Scientific, Inc.) after 1-h incubation. The proteins were then washed and used for mass spectrometry (MS) analysis. The MS analysis included a biotinylated MTO1 pulldown group and streptavidin beads only pulldown groups as negative controls. Briefly, both groups of proteins were eluted and resolved by gel electrophoresis followed by staining with the SilverQuest™ Silver Staining Kit (Thermo Fisher Scientific, Inc.). Then, proteins were excised, de-stained, and digested prior to analysis by using high-performance liquid chromatography with a Thermo Electron LTQ OrbiTrap XL mass spectrometer at Central Laboratory of Shanxi Province People's Hospital. Proteins in MTO1 pulldown group were filtered out with a spectral count less than three, and a cutoff was set up for at least 3-fold peptide enrichment of MTO1 group, as compared with beads only group.

The detailed information for mass spectrometry was as follows: In-gel tryptic digests were fractionated by CapHPLC using a Shimadzu Prominence HPLC system (Shimadzu Corp., Kyoto, Japan) and were introduced directly into the LTQ-Orbitrap XL hybrid MS (Thermo Fisher Scientific, Inc.) equipped with a dynamic nanoelectrospray ion source (Proxeon, Odense, Denmark) and distal coated silica emitters (30 μm i.d., 20 μm tip i.d; New Objective, Woburn, MA, USA). Acidified samples were loaded onto a 120 Å, 3 μm particle size, 300 μm by 10 mm C18-AQ Reprosil-Pur trap column (SGE Australia Pty., Ltd., Clyde, Australia) at 30 μl/min in 98% solvent A [0.1% (v/v) aqueous formic acid] and 2% solvent B [80% (v/v) acetonitrile containing 0.1% (v/v) formic acid] for 3 min at 40˚C, and were subsequently gradient eluted onto a pre-equilibrated self-packed analytical column (Dr Maisch GmbH Reprosil-Pur C18-AQ, 120 Å, 150 μm by 200 mm) using a flow rate of 900 nl/min. The LTQ-Orbitrap was controlled using Xcalibur 2.0 SR1 (Thermo Fisher Scientific, Inc.). Analyses were carried out in data-dependent acquisition mode, whereby the survey full scan mass spectra (m/z 300-2000) were acquired in the Orbitrap FT mass analyser at a resolution of 60,000 (at 400 m/z) after accumulating ions to an automatic gain control target value of $5.0x10^5$ charges in the LTQ mass analyser. MS/MS mass spectra were concurrently acquired on the eight most intense ions in the full scan mass spectra in the LTQ mass analyser to an automatic gain control target value of $3.0x10^4$ charges. Charge state filtering, where unassigned precursor ions were not selected for fragmentation, and dynamic exclusion (repeat count, 1; repeat duration, 30 sec; exclusion list size, 500; and exclusion duration, 90 sec) were used. Fragmentation conditions in the LTQ were: 35% normalised collision energy, activation q of 0.25, isolation width of 3.0 Da, 30 ms activation time, and minimum ion selection intensity 500 counts. Maximum ion injection times were 500 ms for survey full scans and 100 ms for MS/MS.

Fluorescence in situ hybridization analysis (FISH). Nuclear and cytosolic fraction separation was performed using a PARIS kit (Thermo Fisher Scientific, Inc.), and RNA FISH probes were designed and synthesized by Bogu according to the manufacturer's protocol. Briefly, cells were fixed in 4% formaldehyde for 15 min at room temperature and then washed with PBS. The fixed cells were treated with pepsin and dehydrated through ethanol. The air-dried cells were incubated further with 40 nM FISH probe in hybridization buffer. After hybridization, the slide was washed, dehydrated and mounted with Prolong Gold Antifade Reagent with DAPI for detection. The slides were visualized for immunofluorescence with an Olympus fluorescence microscope with an attached CCD camera (Olympus Corporation, Tokyo, Japan).

Immunohistochemistry (IHC). IHC staining was performed on 4 μm-thick TMA slides. Briefly, the slides were deparaffinized and antigen retrieval was then performed in a steam cooker for 1.5 min in 1 mM EDTA. Endogenous peroxidase was quenched by incubating the slides in Peroxidazed I reagent (Biocare Medical, Pacheco, CA, USA) for 5 min and background staining was blocked by incubation in Background Sniper reagent (Biocare Medical) for another 5 min at room temperature. Rabbit anti-Eg5 polyclonal antibody (cat. no. ab61199; Abcam, Cambridge, MA, USA) at 1:150 dilution was used for culture overnight at 4˚C. Universal secondary antibody (cat. no. E043201-6; Goat Anti-Rabbit IgG, 1:5,000; Dako, Santa Clara, CA, USA) was applied for 15 min at room temperature. Diaminobenzidine or 3-amino-9-ethylcarbazole was used as a chromogen and slides were counterstained for 1 min at room temperature with hematoxylin before mounting. The slides were visualized with an Olympus microscope (Olympus Corporation; magnification, x40). ROS1 IHC was scored using a previously described scoring system (21).

Western blotting. Cell lysates were prepared with radioimmunoprecipation buffer containing protease inhibitors (Sigma-Aldrich; Merck KGaA). Protein concentrations were measured with the BCA Protein Assay kit according to the manufacturer's protocol (Beyotime Institute of Biotechnology, Shanghai, China). Equal amounts of protein (25 μg) were separated by 10% sodium dodecyl sulfate-polyacrylamide gel electrophoresis and transferred onto polyvinylidene fluoride membranes (EMD Millipore). Then, the membrane was blocked with 5% (5 g/100 ml) non-fat dry milk in Tris-buffered saline plus Tween (TBS-T) buffer for 2 h at room temperature. The membranes were incubated overnight at 4˚C with a 1:1,000

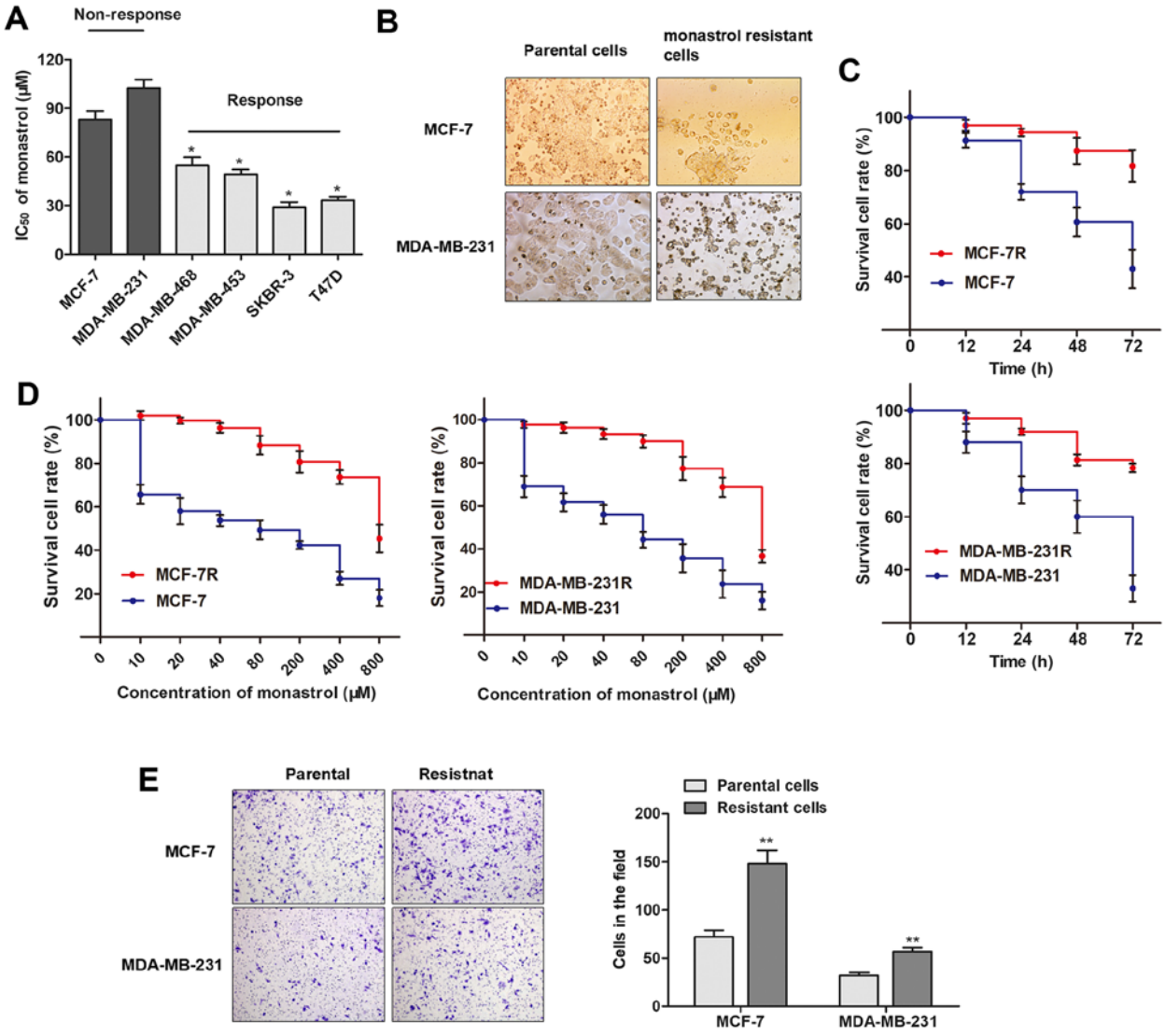

Figure 1. Establishment of monastrol resistant breast cancer cell lines. (A) Determination of monastrol IC_{50} via Cell Counting Kit-8 assay in a panel of breast cancer cell lines (n=3), which were divided into a monastrol-nonresponsive group and a monastrol-responsive group, $^{*}P<0.05$ compared to nonresponsive group. (B) The breast cancer cell line MCF-7 and MDA-MB-231 that had acquired resistance to monastrol at the concentration of 100 μM were built as described in Materials and methods. The representative images were obtained using by using an Olympus microscope, magnification, x20. (C) MCF-7R and MDA-MB-231R cells exhibited elevated cell viability compared with MCF-7 and MDA-MB-231 parental cells when incubated with culture medium containing 100 μM monastrol. (D) Dose-effect curves suggested that the IC_{50} values of monastrol for MCF-7R and MDA-MB-231R cells were significantly higher compared with MCF-7 and MDA-MB-231 cells. (E) Transwell assay revealed that a significantly increased number of monastrol resistant cells were observed to migrate through the collagen membrane when compared with the parental cells, $^{*}P<0.05$; $^{**}P<0.01$ compared to parental cells.

solution of antibodies: anti-Eg5 (Abcam; cat. no. ab61199) and anti-β-actin (Abcam; cat. no. ab8227). The horseradish peroxidase-conjugated anti-rabbit antibody (cat. no. #7074; 1:5,000; Cell Signaling Technology, Danvers, MA, USA) was used as a secondary antibody for immunostaining for 1 h at room temperature. Immunoblots were visualized using Immobilon™ Western Chemiluminescent HRP Substrate (EMD Millipore). Densitometry was performed by using ImageJ software version 1.51r (National Institutes of Health, Bethesda, MD, USA) (22).

Cell invasion assay. A Transwell invasion assay was performed to evaluate the invasive ability of breast cancer cells. Briefly, 100 μl matrigel (Ambion; Thermo Fisher Scientific, Inc.) was firstly added onto the bottom of the transwell chamber (24-well insert; 8-mm pore size; Corning Costar Corp., Corning, NY, USA), then $1x10^5$ cells in reduced serum medium (Opti-MEM; Gibco; Thermo Fisher Scientific, Inc.) were placed on the coated membrane in the chamber. DMEM supplemented with 10% FBS was placed in the bottom wells as chemoattractant. After 24 h, cells that did not migrate were removed from the top side of the inserts with a cotton swab. Cells that migrated through the permeable membrane were fixed in 4% paraformaldehyde for 15 min at room temperature, stained with crystal violet for 5 min at room temperature, and counted under a microscope (Olympus Corporation) at magnification, x20 in 5 random fields in each well.

Statistical analysis. The Mann-Whitney U test or Kruskal-Wallis test (post hoc Mann-Whitney U test with Bonferroni's correction) as used for evaluating the difference among different cell groups. The survival curves of breast cancer cells

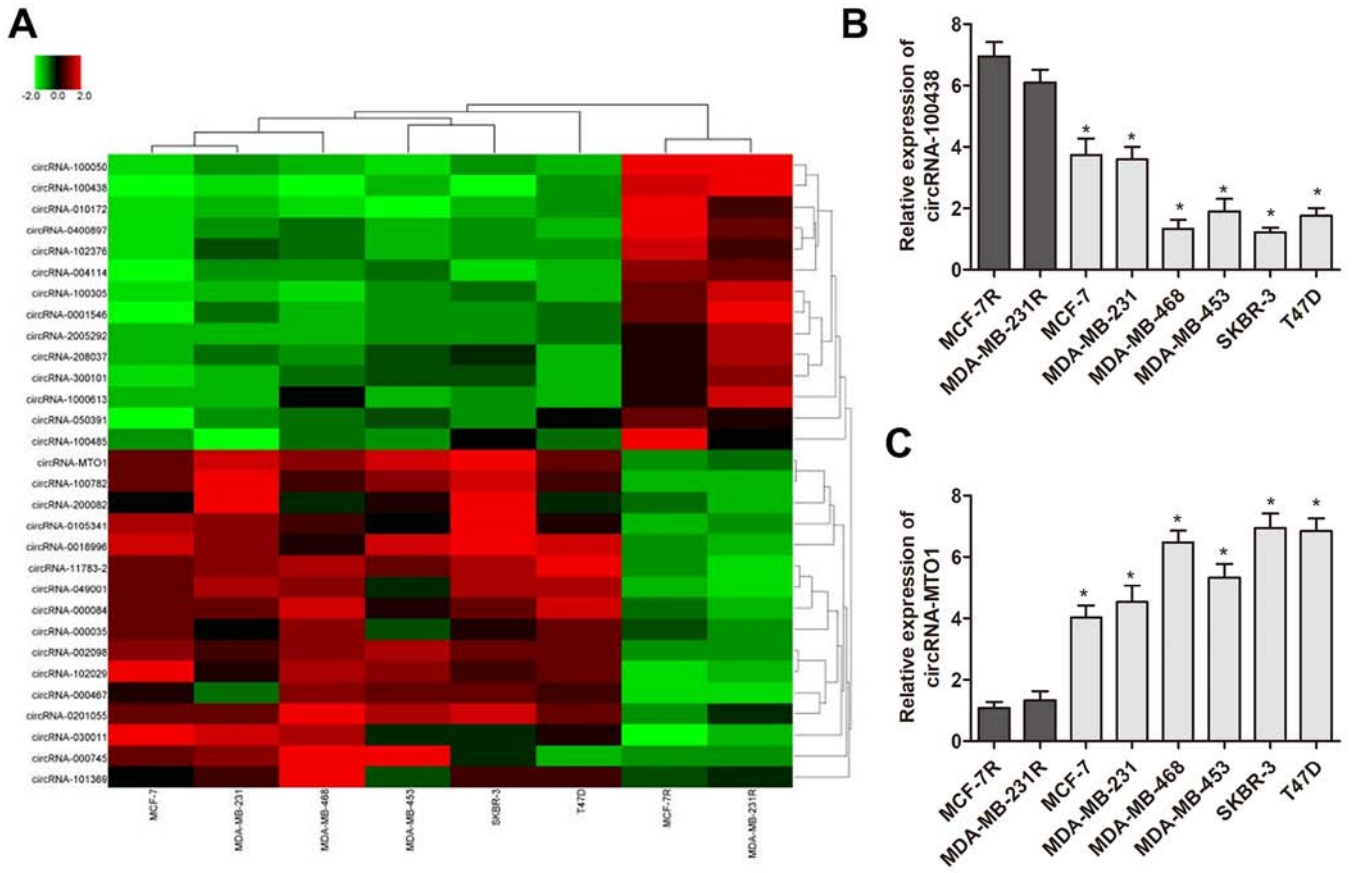

Figure 2. Deregulated circRNAs in monastrol resistant cells. (A) The 30 most deregulated circRNAs (15 upregulated and 15 downregulated) between chemoresistant cells and parental cells were presented as a heat map via circRNA microarray. Reverse transcription-quantitative polymerase chain reaction was performed to reveal the expression level of (B) circRNA-100438 and (C) circRNA-MTO1 from six non-resistant cell lines and two monastrol resistant cell lines. *P<0.05 compared to MCF-7R and MDA-MB-231R cells, respectively. circRNA, circular RNA.

were estimated via the Kaplan-Meier method, and the difference in survival rate was analyzed using the log-rank testing. All statistical analyses were performed with SPSS software, version 17.0 (SPSS Inc., Chicago, IL, USA). The package plots and function heatmap in R software (http://www.R-project.org/) were used for mapping. Error bars in figures represent standard deviation. P<0.05 was considered to indicate a statistically significant difference.

Results

Acquisition of monastrol resistance induces elevated cell viability in breast cancer cells. A panel of breast cancer cell lines was divided into two groups according to their response to monastrol (Fig. 1A). The two cell lines that exhibited little response to monastrol treatment, MCF-7 and MDA-MB-231, were constantly exposed to a high concentration of monastrol (100 μM) to establish the monastrol-resistant cell lines, MCF-7R and MDA-MB-231R. As presented in Fig. 1B, the establishment of monastrol resistant cells induced specific morphological changes, including loss of cell polarity, increased intercellular separation, and increased formation of pseudopodia. Furthermore, MCF-7R and MDA-MB-231R cells exhibited elevated cell viability compared with the parental cells when incubated with culture medium containing 100 μM concentration of monastrol for 48 h (Fig. 1C). The concentration-effect curve indicated that the IC_{50} of monastrol (48 h) on MCF-7R was 726.3 μM, while the IC_{50} of monastrol on MCF-7 was 81.5 μM, which indicated that monastrol resistance for MCF-7R cells was 8.91 times higher compared with MCF-7 cells. Similarly, the MDA-MB-231R was 8.49 times the ability of monastrol resistance of MDA-MB-231 (607.9/71.6 μM, Fig. 1D). At 48 h, a significantly increased number of chemoresistant cells were observed to migrate through the collagen membrane compared with parental cells (Fig. 1E), indicating an increased cell migratory ability. To conclude, the monastrol resistant cell lines were successfully established.

Monastrol resistance induces downregulation of circRNA-MTO1 in breast cancer cells. To identify specific circRNAs that have important roles of monastrol resistance, circRNA microarray analysis was performed using two monastrol resistant cell lines and six non-resistant breast cancer cell lines. This assay identified 398 circRNAs which were deregulated between the two cell types. To further identify the specific circRNAs, the results were narrowed to 30 circRNAs (15 upregulated and 15 downregulated) which exhibited the most altered expression levels (presented in heat map, Fig. 2A). RT-qPCR was then performed to verify the expression pattern of these 30 circRNAs in monastrol resistant and parental cells. As presented in Fig. 2B and C, two circRNAs were identified with a consistent expression gap between monastrol resistant

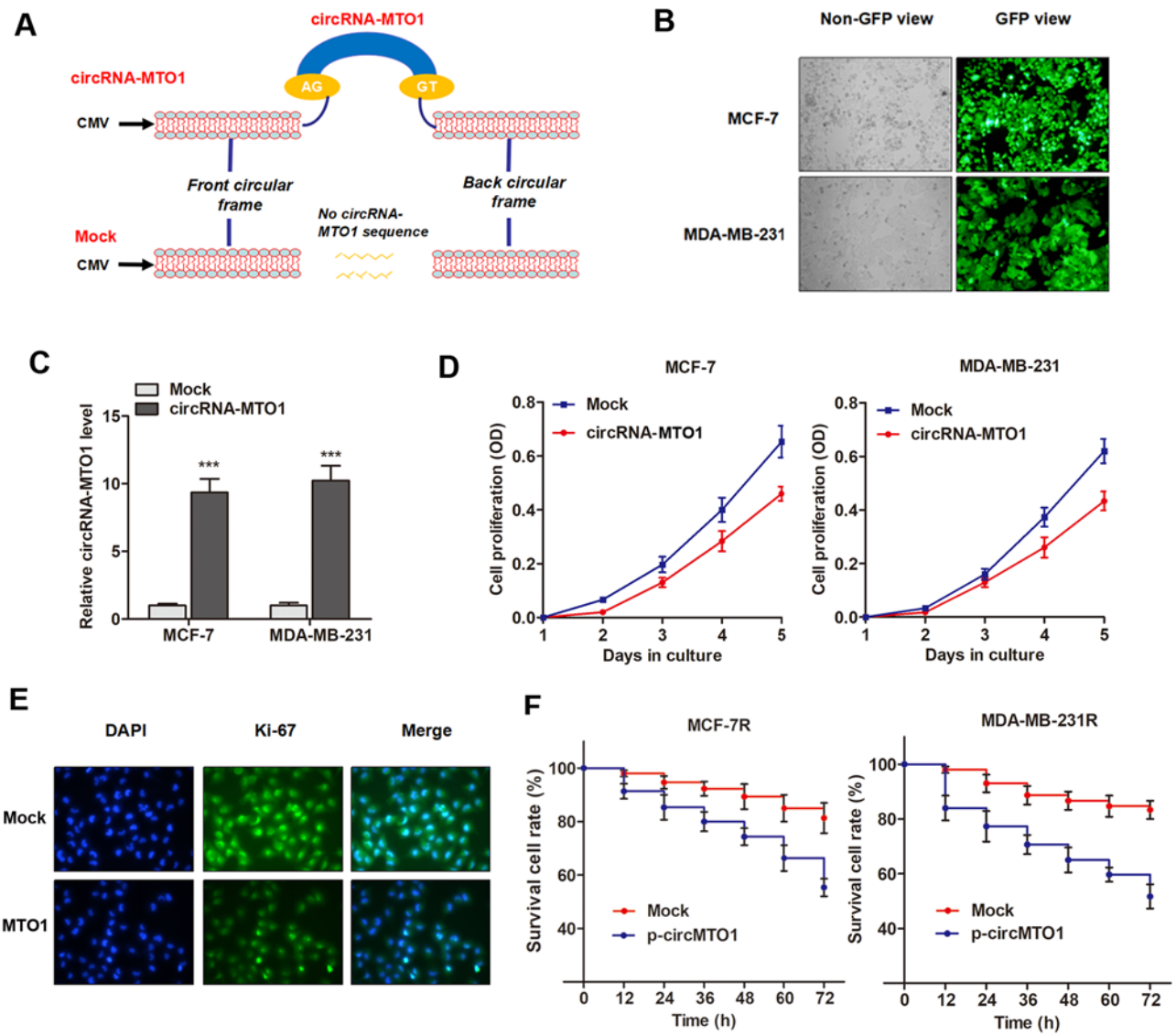

Figure 3. Functional role of circRNA-MTO1 in breast cancer tumorigenesis. (A) The analogue diagram of pattern of circRNA-MTO1 and controlled vector are shown. (B) The oligonucleotides labeled with GFP green fluorescence were successfully transfected. (C) circRNA-MTO1 expression level was significantly increased in cells transfected with MTO1 vectors, ***P<0.001 vs. Mock group. (D) circRNA-MTO1 inhibited viability of MCF-7 and MDA-MB-231 cells determined by Cell Counting Kit-8 assay. (E) Immunofluorescence assay suggested that overexpression of circRNA-MTO1 inhibited the expression of cell proliferation marker, Ki-67. (F) Cell viability was significantly damaged when circRNA-MTO1 was overexpressed in MCF-7R and MDA-MB-231R cells compared with control. circRNA, circular RNA; GFP, green fluorescent protein.

cells and parental cells as compared with microarray data (P<0.05), including circRNA-MTO1 (hsa-circRNA-007874) and circRNA-100438. In addition, the preliminary results demonstrated that silencing of circRNA-100438 had no significant effect on breast cancer cell viability (data not shown), while silencing of circRNA-MTO1 significantly increased cell viability. Therefore, the high percentage of circRNA-MTO1 decrease in monastrol-resistant cells led to further investigation of the functional role of circRNA-MTO1 in breast cancer resistance.

Overexpression of circRNA-MTO1 inhibits cell viability and reverses monastrol resistance. The present study investigated the functional role of MTO1 in cell viability and chemoresistance. To determine whether the upregulation of MTO1 could inhibit cell viability and reverse monastrol resistance of breast cancer cells, the specific plasmid of circRNA-MTO1 was designed from MCF-7 cells and cloned into the specific vector (Fig. 3A), then MTO1 was upregulated via the transfection of pcDNA3.1-MTO1 vectors (Fig. 3B and C). CCK-8 assay revealed that enhanced MTO1 expression inhibited the viability of breast cancer cells compared with control (Fig. 3D). This data was further validated by the detection of Ki-67 expression, a known biomarker of cell viability, in MCF-7 cells (Fig. 3E). However, MTO1 had little effect on cell apoptosis (data not shown), indicating that MTO1 may regulate monastrol resistance by influencing cell viability. Notably, monastrol resistant cells with enhanced expression of MTO1 were more sensitive to the treatment of monastrol at the concentration of 100 nM (Fig. 3F), indicating that MTO1 partially reversed monastrol resistance.

circRNA-MTO1 promotes monastrol-induced cytotoxicity in breast cancer cells. By using the MCF-7 and MDA-MB-231

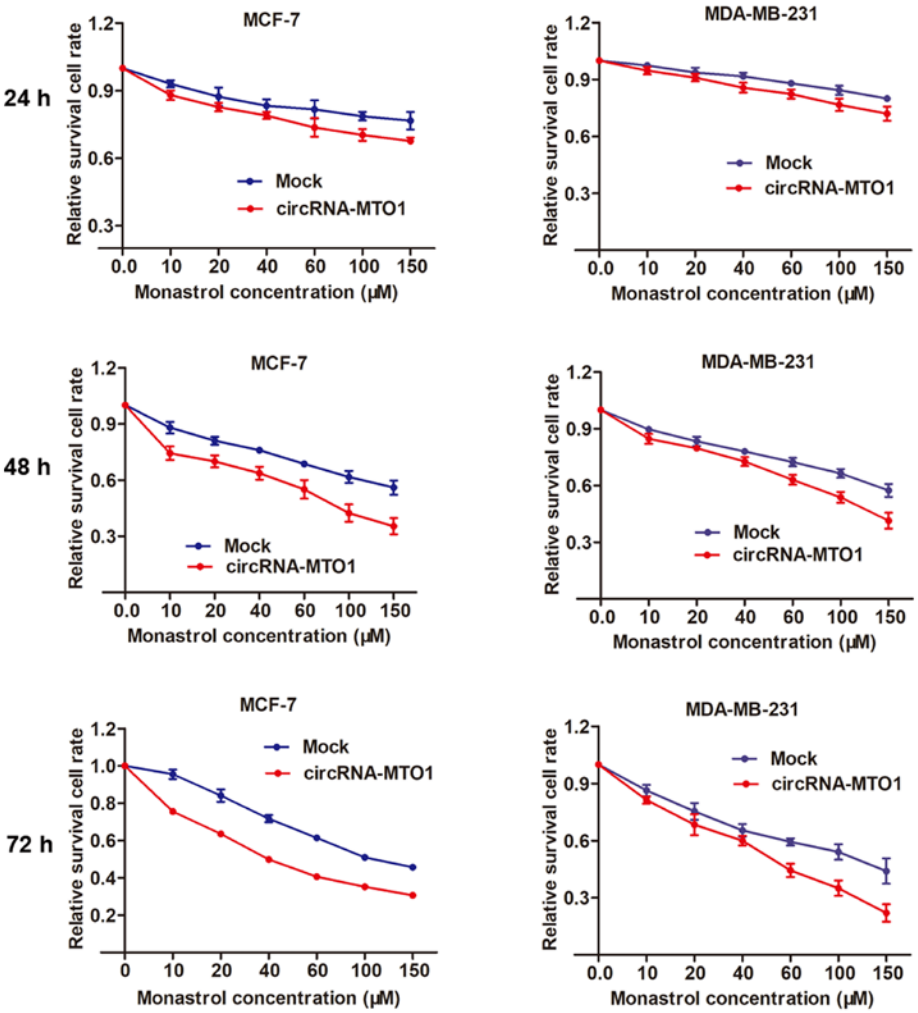

Figure 4. circRNA-MTO1 promotes monastrol-induced cytotoxicity. The breast cancer cell survival rate was measured with a concentration gradient of 10, 20, 40, 60, 100, 150 μM monastrol for 24, 48 and 72 h, and the relative cell absorbance in the absence of monastrol was set as the start 100% point. circRNA, circular RNA.

parental cells, the present study then investigated whether MTO1 enhances monastrol cytotoxicity. After being transfected with MTO1 overexpression vector or negative control, MCF-7 and MDA-MB-231 cells were incubated without monastrol or with a concentration gradient of 10, 20, 40, 60, 100, 150 μM monastrol for 24, 48 and 72 h. Then, a dose-effect curve was constructed based on the viability of cells. The graph showed that enhanced expression of MTO1 was followed by increased cell death compared with the negative control in monastrol treated cells at different concentrations (Fig. 4).

circRNA-MTO1 suppresses cell viability and reverses monastrol resistance through targeting Eg5 protein. It is well known that monastrol exerts the tumor-suppressive function mainly through blockage of mitotic kinesin Eg5, which is required for the formation of a bipolar spindle (8). Inhibition of Eg5 has gained primary attention as an alternative strategy to interfere with spindle function. As the synergistic effect of circRNA-MTO1 with monastrol treatment was verified, the present study then investigated whether circRNA-MTO1 targets Eg5 protein, thereby inducing a tumor suppressive effect. Western blotting revealed that Eg5 protein was inhibited by overexpression of MTO1 in the two breast cancer cell lines (Fig. 5A). Notably, MTO1 did not affect the Eg5 mRNA level, suggesting that MTO1 may regulate Eg5 at a post transcriptional level (Fig. 5B).

Next, it was determined whether Eg5 plays a causal role during the MTO1-regulated cell viability and monastrol resistance. Eg5 was upregulated by transfection of specific Eg5-containing plasmid (Fig. 5C). Enhanced expression of Eg5 significantly abrogated the decreased cell growth and reversed the chemo response to monastrol induced by MTO1 overexpression in MCF-7R and MDA-MB-231R cells (Fig. 5D and E). Collectively, the results suggested that MTO1 regulates cell viability and monastrol resistance through inhibiting Eg5 levels at the post-transcriptional level.

circRNA-MTO1 sequesters TRAF4 from binding to Eg5 gene. Furthermore, the present study investigated how circRNA-MTO1 targets and inhibits the expression of Eg5 gene. By treating with cycloheximide (CHX), a protein synthesis inhibitor, it was revealed that MTO1 did not affect the protein stability of Eg5 (Fig. 6A), indicating that MTO1 may affect the protein level of Eg5 at post-transcriptional level. Subsequently, RNA-pull down experiments were performed followed by mass spectrometry to search for the MTO1-associated proteins.

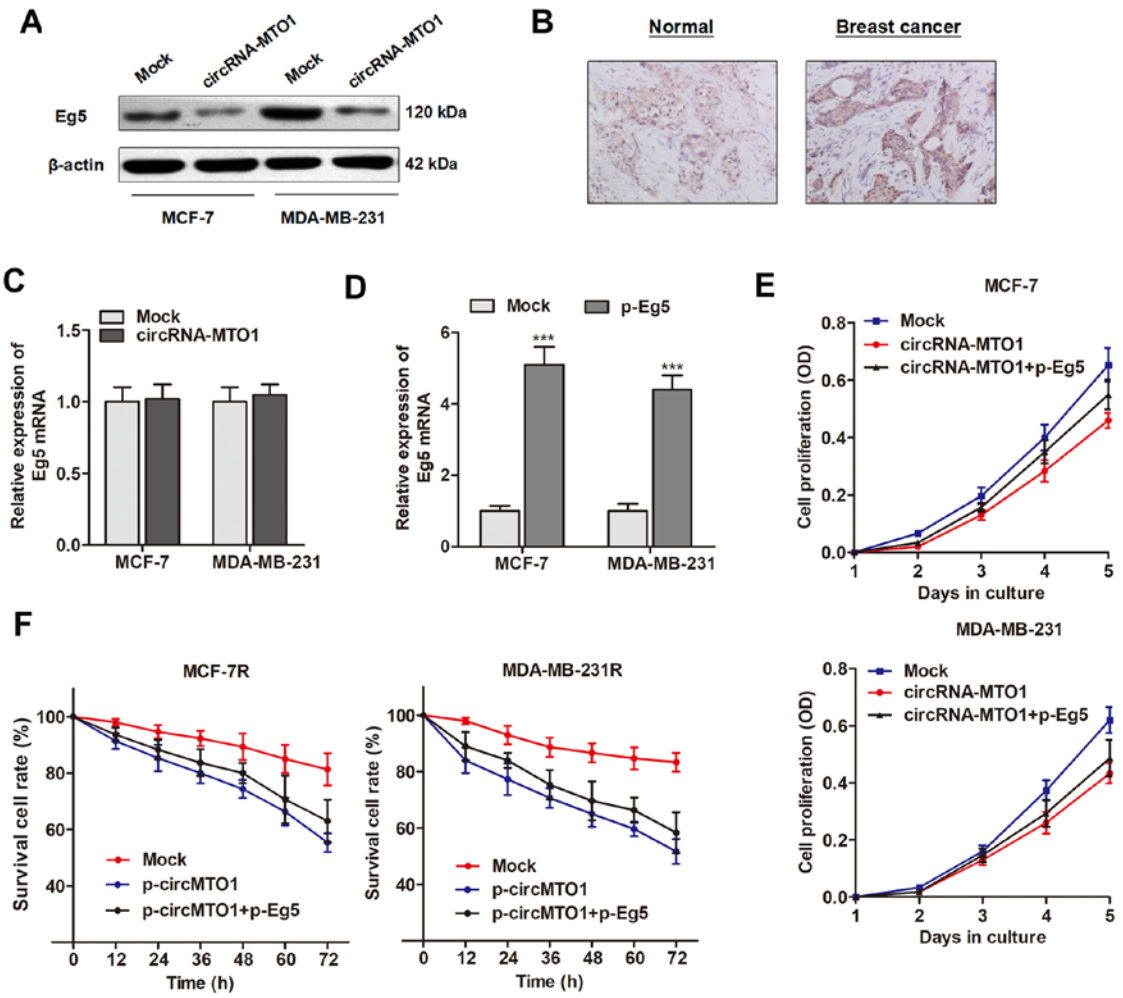

Figure 5. Eg5 protein is a functional target of circRNA-MTO1. (A) Eg5 protein was downregulated by overexpression of circRNA-MTO1 in MCF-7 and MDA-MB-231 cells by western blotting. (B) Reverse transcription-quantitative polymerase chain reaction revealed that circRNA-MTO1 had no effect on Eg5 mRNA expression level. (C) Eg5 was upregulated via the transfection of specific overexpression vector, $^{***}P<0.001$ vs. Mock group. (D) Overexpression of Eg5 abrogated the circRNA-MTO1-induced suppression of cell viability. (E) Overexpression of Eg5 partially reversed the effect of MTO1 on monastrol resistance. circRNA, circular RNA.

As presented in Table I, a list of correlative MTO1-associated proteins were identified. Then, these potential regulator genes were evaluated to identify the specific protein that may activate Eg5 at the post-transcriptional level. The assays validated TRAF4 as a potential interacting protein of MTO1. It has previously been reported that TRAF4 is an (A+U)-rich elements (AREs)-binding protein, and can interact with ARE areas within the 3' UTR of target gene and activates translation without influencing the mRNA level (23). The present study then localized the expression pattern of MTO1 and observed that MTO1 was expressed in both nucleus and cytoplasm of MCF-7 parental cells (Fig. 6B), however, monastrol resistance significantly increased the proportion of MTO1 localization in the nucleus (Fig. 6C). In addition, the RIP assay revealed an interaction between MTO1 and TRAF4 protein in MCF-7 cells; however, the enrichment between MTO1 and TRAF4 protein was suppressed in MCF-7R cells (Fig. 6D). MTO1 overexpression decreased the interaction between TRAF4 and Eg5 gene in MCF-7R cells (Fig. 6E). Taken together, these data indicated that MTO1 serves as a competing endogenous RNA (ceRNA) binding to TRAF4, and therefore inhibits Eg5 protein level and reverses monastrol resistance.

Discussion

Extensive efforts in the past have contributed to the understanding of both molecular and cellular mechanisms of action of chemoresistance, one of the major causes for the failure of treatment in advanced cancer types. However, little progress has been regarding this issue (24). Thus, novel molecular signatures seem to hold great promise in tumor characterization and could be used as potential prognostic markers and treatment targets. The present study established monastrol resistant cell lines, and sought to find potential interactions between monastrol resistance and a novel group of gene regulators, circRNAs. First, the downregulation of circRNA-MTO1 in monastrol resistant cells was identified by utilizing microarray analysis. Then, *in vitro* investigations suggested that circRNA-MTO1 inhibited cell viability, and reversed monastrol resistance of breast cancer cells by inhibiting Eg5 protein via TRAF4.

Monastrol is a reversible, cell-permeable, small molecule that selectively inhibits the plus-end-directed Kinesin-5 family member, Eg5 (25,26), a microtubule-based motor protein that is required for the formation and maintenance of the bipolar spindle (27). Monastrol treatment of dividing cells results in

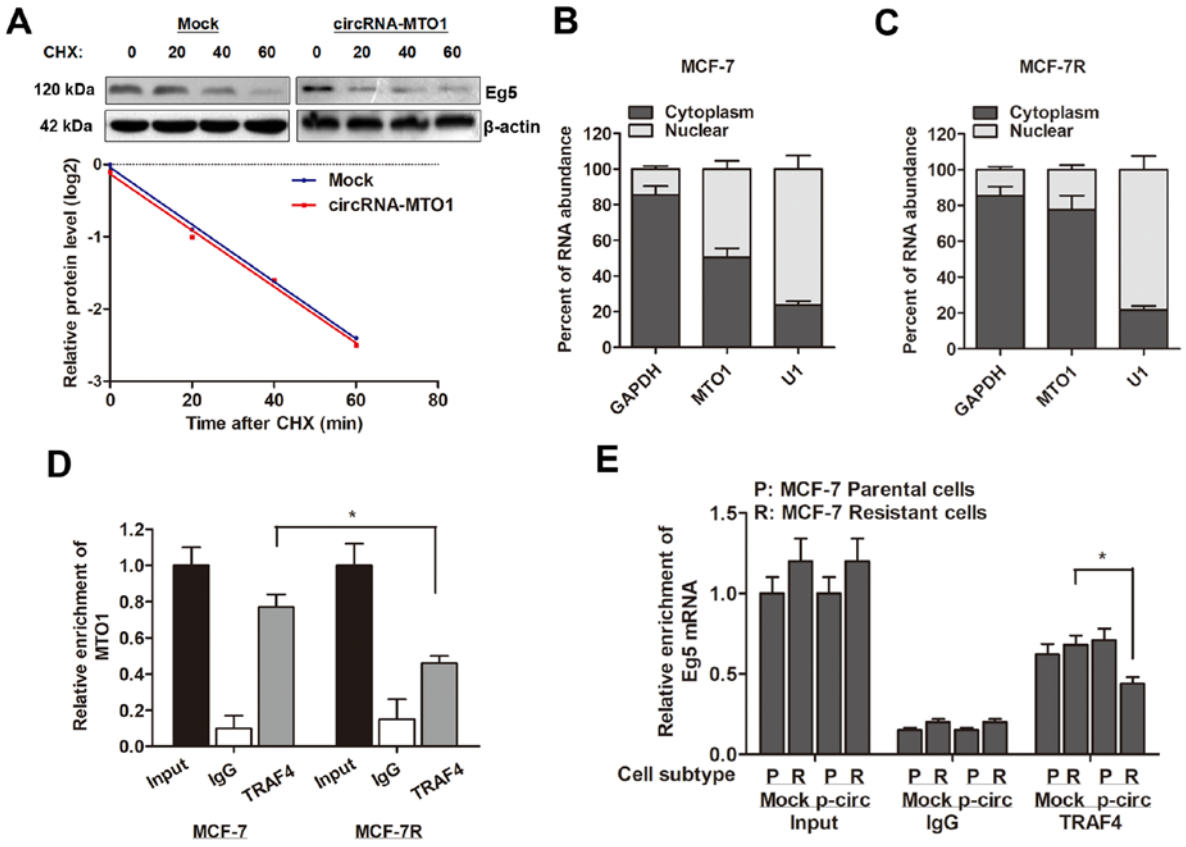

Figure 6 circRNA-MTO1 sequesters TRAF4 from binding to Eg5 gene. (A) Control mock or circRNA-MTO1 transfected MCF-7R cells were cultured with medium containing 20 μg/ml cycloheximide (CHX) for 0-60 min, then subjected to western blotting. Fractionation experiments revealed that MTO1 was localized in both cytoplasm and nucleus in (B) MCF-7 parental cells, however, (C) monastrol resistance increased cytoplasmic localization of MTO1. (D) Whole-cell lysates were obtained from MCF-7 and MCF-7R cells, then RIP experiments were performed using an TRAF-4 antibody to immunoprecipitate RNA and primers to detect MTO1. (E) RIP assay was performed to detect the effect of circRNA-MTO1 on the interaction between Eg5 and TRAF4 in both MCF-7 and MCF-7R cells. *P<0.05. circRNA, circular RNA; TRAF4, tumor necrosis factor receptor associated factor 4.

spindle collapse and cell cycle arrest with a monastrol spindle, which is similar to the phenotype observed when Eg5 is inhibited by anti-Eg5 antibodies. The anticancer effect of monastrol in breast cancer patients has been frequently reported, and a chemoresistance has also been revealed (28). The existence of circular form RNAs in body fluid was firstly reported by Sanger *et al* in 1976 (29), demonstrating that this type of single-stranded closed circular RNA is stably expressed from viroid to certain higher species, such as human beings. With the development of gene investigations, it is recognized that circRNAs are widely expressed in human cells, and their expression levels can be 10-fold or higher compared to their linear isomers. The two most important properties of circRNAs are highly conserved sequences and a high degree of stability in mammalian cells (30). Compared with other noncoding RNA, such as microRNA (miRNA) and long noncoding RNA (lncRNA), these properties provide circRNAs with the potential to become ideal biomarkers in the diagnosis and prognosis of cancers (31,32).

To date, only a few circRNAs have been explored. The present study identified a circular RNA termed circRNA-MTO1 that was significantly downregulated in monastrol resistant cells and was associated with chemosensitivity. MTO1, a gene conserved in all eukaryotes, encodes one of the two subunits of the enzyme that catalyzes the 5-carboxymethylaminomethylation (mnm5s2U34) of the wobble uridine base in the mitochondrial tRNA specific to Gln, Glu, Lys, Leu (UUR), and possibly Trp (33,34). The biological role of its circular form, circRNA-MTO1 was reported only once. Han *et al* (20) demonstrated that circRNA-MTO1 may serve as a competing endogenous RNA (ceRNA) through binding to miR-9, thereby inducing the suppression of hepatocellular progression. The study identified circRNA-MTO1 as one circRNA significantly downregulated in HCC tissues, and HCC patients with low circRNA-MTO1 expression had shortened survival. In addition, circRNA-MTO1 suppresses HCC progression by acting as the sponge of oncogenic miR-9 to promote downstream p21 gene expression levels. The results of the present study indicated that MTO1 may also serve as a tumor suppressor in breast cancer. However, another identified circRNA, circRNA-100438, demonstrated no effect on monastrol resistance, and whether it participates in the oncogenic process remains unknown. Thus, the functional role of circRNA-100438 requires further investigation in future studies to verify whether it regulates progression of breast cancer as well as other cancer types.

The functional role of MTO1 in breast cancer progression and chemoresistance was then evaluated. To comprehensively investigate the effect of MTO1 in chemoresistance, the present study established two monastrol resistant cell lines, MCF-7R and MDA-MB-231R. Consistent with the study by Han *et al*, it was validated that MTO1 plays a tumor-suppressor role, including the inhibition of cell growth, and the promotion of

Table I. Identification of circRNA-MTO1 binding proteins by mass spectrometry.

Protein	Beads	MTO1	Ratio (MTO1/Beads)
TRAF4	0	3	NA
U2AF1	1	3	3
NKRF	0	3	NA
EF1D	0	3	NA
AIMP2	0	3	NA
ROA0	0	3	NA
RO60	0	3	NA
ARP2	0	3	NA
STT3B	0	3	NA
PCH2	1	3	3
MRP1	0	3	NA
LAS1L	0	3	NA
ARF6	1	3	3
PLST	0	3	NA
PSAL	0	3	NA
TTL12	0	3	NA
ERLN1	0	3	NA
NSF	0	3	NA
AKAP8	0	3	NA
GSTO1	0	3	NA
AP1B1	0	3	NA
DPM1	0	3	NA
PSDE	1	3	3
KTN1	1	3	3

Beads, spectral counts of proteins in beads only group; MTO1, spectral counts of proteins in MTO1 group; Ratio (MTO1/Beads), spectral count ratio of proteins comparing MTO1 group to beads only group; NA, not available.

monastrol chemosensitivity. Furthermore, the present study identified the mechanism by which MTO1 serves a tumor-suppressive role. Eg5 protein is well recognized as a direct target of monastrol and MTO1 has a synergistic function with monastrol, therefore whether MTO1 reverses monastrol resistance through targeting Eg5 protein was investigated. The expression of Eg5 is closely associated with cell viability and cancer. Overexpression of Eg5 has been observed in bladder cancer (35) and pancreatic cancer (36). Furthermore, transgenic mice overexpressing Eg5 are prone to developing a variety of tumors (37). These and other observations favor Eg5 as an attractive target for chemotherapy. In addition, the *in vitro* experiments verified that MTO1 inhibited Eg5 protein level, however, MTO1 had little influence on the mRNA level of Eg5 gene. In addition, the data obtained following treatment of CHX indicated that MTO1 did not affect the Eg5 protein stability.

To further explore how MTO1 regulates the protein level of Eg5, an RNA pulldown assay and mass spectrometry were performed, and it was observed that MTO1 physically interacted with the TRAF4 gene. Furthermore, the proportion of MTO1 localized in the cytoplasm was enhanced in cells resistant to monastrol treatment. In addition, monastrol resistance elevated the physical interaction between MTO1 and the TRAF4 gene. As one of the important members of the TRAF family of proteins, TRAF4 was initially isolated from breast carcinomas and identified as the first member of the TRAFfamily to be upregulated in human carcinomas (38). TRAF family members mainly function in the immune system, where they mediate signaling via tumor necrosis factor receptors and interleukin-1/Toll-like receptors (39,40). TRAF4 has been considered as an oncogene as it is overexpressed in a wide range of human malignancies, including breast cancer, lung cancer, colon adenocarcinomas, melanomas, neurogenic tumors and lymphomas (41). Accumulating evidence indicates that TRAF4 plays a critical role in breast cancer, such as antiapoptosis, and promotes cell migration (42). The data revealed a circRNA network that that revealed that under conditions of monastrol resistance, circRNA-MTO1 interacts with TRAF4, and may serve as a ceRNA to repress TRAF4 from binding to the Eg5 gene, leading to suppression of Eg5 protein levels, prevention of cell viability and reversal of monastrol resistance.

In conclusion, the results of the present study indicated a circRNA-involved regulatory pattern to mediate Eg5 protein expression during monastrol resistance. First, monastrol resistance induced downregulated circRNA-MTO1 expression in breast cancer cells. Second, overexpression of MTO1 repressed viability and reversed monastrol resistance through inhibiting Eg5 protein level and associating with TRAF4. Therefore, circRNA-MTO1 may be a functional regulatory factor of breast cancer, and restoration of MTO1 levels could be a future direction to overcome breast cancer chemoresistance.

Acknowledgements

Not applicable.

Funding

The present study was supported by the Basic Research Projects of Shandong Province (grant no. 201601D202100).

Availability of data and materials

The analyzed data sets generated during the study are available from the corresponding author on reasonable request.

Authors' contributions

YL and YD designed this work and created a draft of the manuscript; YL, LZ and LS prepared the reagents and kits and performed the *in vitro* experiments; YL and JL analyzed and interpreted the original results, and performed statistical analysis; YL and YD revised and approved the final version of the manuscript. All authors have read and approved the final manuscript.

Ethics approval and consent to participate

The study protocol was approved by the Ethics Committee of Shanxi Province People's Hospital (Taiyuan, China).

Patient consent for publication

Not applicable.

Competing interests

The authors declare that they have no competing interests.

References

1. Torre LA, Bray F, Siegel RL, Ferlay J, Lortet-Tieulent J and Jemal A: Global cancer statistics, 2012. CA Cancer J Clin 65: 87-108, 2015.
2. Zhang B, Beeghly-Fadiel A, Long J and Zheng W: Genetic variants associated with breast-cancer risk: Comprehensive research synopsis, meta-analysis, and epidemiological evidence. Lancet Oncol 12: 477-488, 2011.
3. Calaf GM, Zepeda AB, Castillo RL, Figueroa CA, Arias C, Figueroa E and Farías JG: Molecular aspects of breast cancer resistance to drugs (review). Int J Oncol 47: 437-445, 2015.
4. Chen W, Zheng R, Zeng H and Zhang S: The updated incidences and mortalities of major cancers in China, 2011. Chin J Cancer 34: 502-507, 2015.
5. Quasthoff S and Hartung HP: Chemotherapy-induced peripheral neuropathy. J Neurol 249: 9-17, 2002.
6. Mayer TU, Kapoor TM, Haggarty SJ, King RW, Schreiber SL and Mitchison TJ: Small molecule inhibitor of mitotic spindle bipolarity identified in a phenotype-based screen. Science 286: 971-974, 1999.
7. Kapoor TM, Mayer TU, Coughlin ML and Mitchison TJ: Probing spindle assembly mechanisms with monastrol, a small molecule inhibitor of the mitotic kinesin, Eg5. J Cell Biol 150: 975-988, 2000.
8. Maliga Z, Kapoor TM and Mitchison TJ: Evidence that monastrol is an allosteric inhibitor of the mitotic kinesin Eg5. Chem Biol 9: 989-996, 2002.
9. Blangy A, Lane HA, d'Hérin P, Harper M, Kress M and Nigg EA: Phosphorylation by p34cdc2 regulates spindle association of human Eg5, a kinesin-related motor essential for bipolar spindle formation in vivo. Cell 83: 1159-1169, 1995.
10. Sharp DJ, Yu KR, Sisson JC, Sullivan W and Scholey JM: Antagonistic microtubule-sliding motors position mitotic centrosomes in Drosophila early embryos. Nat Cell Biol 1: 51-54, 1999.
11. Sorek R and Cossart P: Prokaryotic transcriptomics: A new view on regulation, physiology and pathogenicity. Nat Rev Genet 11: 9-16, 2010.
12. Memczak S, Jens M, Elefsinioti A, Torti F, Krueger J, Rybak A, Maier L, Mackowiak SD, Gregersen LH, Munschauer M, *et al*: Circular RNAs are a large class of animal RNAs with regulatory potency. Nature 495: 333-338, 2013.
13. Jeck WR, Sorrentino JA, Wang K, Slevin MK, Burd CE, Liu J, Marzluff WF and Sharpless NE: Circular RNAs are abundant, conserved, and associated with ALU repeats. RNA 19: 141-157, 2013.
14. Li JH, Liu S, Zhou H, Qu LH and Yang JH: starBase v2.0: Decoding miRNA-ceRNA, miRNA-ncRNA and protein-RNA interaction networks from large-scale CLIP-Seq data. Nucleic Acids Res 42D: D92-D97, 2014.
15. Huang G, Li S, Yang N, Zou Y, Zheng D and Xiao T: Recent progress in circular RNAs in human cancers. Cancer Lett 404: 8-18, 2017.
16. Lasda E and Parker R: Circular RNAs: Diversity of form and function. RNA 20: 1829-1842, 2014.
17. Du WW, Yang W, Liu E, Yang Z, Dhaliwal P and Yang BB: Foxo3 circular RNA retards cell cycle progression via forming ternary complexes with p21 and CDK2. Nucleic Acids Res 44: 2846-2858, 2016.
18. Xu SY, Huang X and Cheong KL: Recent advances in marine algae polysaccharides: Isolation, structure, and activities. Mar Drugs 15: 15, 2017.
19. Livak KJ and Schmittgen TD: Analysis of relative gene expression data using real-time quantitative PCR and the 2(-Delta Delta C(T)) Method. Methods 25: 402-408, 2001.
20. Han D, Li J, Wang H, Su X, Hou J, Gu Y, Qian C, Lin Y, Liu X, Huang M, *et al*: Circular RNA circMTO1 acts as the sponge of microRNA-9 to suppress hepatocellular carcinoma progression. Hepatology 66: 1151-1164, 2017.
21. Remmele W and Stegner HE: [Recommendation for uniform definition of an immunoreactive score (IRS) for immunohistochemical estrogen receptor detection (ER-ICA) in breast cancer tissue]. Pathologe 8: 138-140, 1987.
22. Schindelin J, Rueden CT, Hiner MC and Eliceiri KW: The ImageJ ecosystem: An open platform for biomedical image analysis. Mol Reprod Dev 82: 518-529, 2015.
23. Zhang L, Zhou F, García de Vinuesa A, de Kruijf EM, Mesker WE, Hui L, Drabsch Y, Li Y, Bauer A, Rousseau A, *et al*: TRAF4 promotes TGF-β receptor signaling and drives breast cancer metastasis. Mol Cell 51: 559-572, 2013.
24. Wang Z, Wang N, Li W, Liu P, Chen Q, Situ H, Zhong S, Guo L, Lin Y, Shen J, *et al*: Caveolin-1 mediates chemoresistance in breast cancer stem cells via β-catenin/ABCG2 signaling pathway. Carcinogenesis 35: 2346-2356, 2014.
25. DeBonis S, Simorre JP, Crevel I, Lebeau L, Skoufias DA, Blangy A, Ebel C, Gans P, Cross R, Hackney DD, *et al*: Interaction of the mitotic inhibitor monastrol with human kinesin Eg5. Biochemistry 42: 338-349, 2003.
26. Yan Y, Sardana V, Xu B, Homnick C, Halczenko W, Buser CA, Schaber M, Hartman GD, Huber HE and Kuo LC: Inhibition of a mitotic motor protein: Where, how, and conformational consequences. J Mol Biol 335: 547-554, 2004.
27. Sawin KE, LeGuellec K, Philippe M and Mitchison TJ: Mitotic spindle organization by a plus-end-directed microtubule motor. Nature 359: 540-543, 1992.
28. Sashidhara KV, Avula SR, Sharma K, Palnati GR and Bathula SR: Discovery of coumarin-monastrol hybrid as potential antibreast tumor-specific agent. Eur J Med Chem 60: 120-127, 2013.
29. Sanger HL, Klotz G, Riesner D, Gross HJ and Kleinschmidt AK: Viroids are single-stranded covalently closed circular RNA molecules existing as highly base-paired rod-like structures. Proc Natl Acad Sci USA 73: 3852-3856, 1976.
30. Guo JU, Agarwal V, Guo H and Bartel DP: Expanded identification and characterization of mammalian circular RNAs. Genome Biol 15: 409, 2014.
31. Huang YS, Jie N, Zou KJ and Weng Y: Expression profile of circular RNAs in human gastric cancer tissues. Mol Med Rep 16: 2469-2476, 2017.
32. Nair AA, Niu N, Tang X, Thompson KJ, Wang L, Kocher JP, Subramanian S and Kalari KR: Circular RNAs and their associations with breast cancer subtypes. Oncotarget 7: 80967-80979, 2016.
33. Suzuki T, Nagao A and Suzuki T: Human mitochondrial tRNAs: Biogenesis, function, structural aspects, and diseases. Annu Rev Genet 45: 299-329, 2011.
34. Wang X, Yan Q and Guan MX: Combination of the loss of cmnm5U34 with the lack of s2U34 modifications of tRNALys, tRNAGlu, and tRNAGln altered mitochondrial biogenesis and respiration. J Mol Biol 395: 1038-1048, 2010.
35. Ding S, Xing N, Lu J, Zhang H, Nishizawa K, Liu S, Yuan X, Qin Y, Liu Y, Ogawa O, *et al*: Overexpression of Eg5 predicts unfavorable prognosis in non-muscle invasive bladder urothelial carcinoma. Int J Urol. 18: 432-438, 2011.
36. Liu M, Wang X, Yang Y, Li D, Ren H, Zhu Q, Chen Q, Han S, Hao J and Zhou J: Ectopic expression of the microtubule-dependent motor protein Eg5 promotes pancreatic tumourigenesis. J Pathol 221: 221-228, 2010.
37. Wang Y, Wu X, Du M, Chen X, Ning X, Chen H, Wang S, Liu J, Liu Z, Li R, *et al*: Eg5 inhibitor YL001 induces mitotic arrest and inhibits tumor proliferation. Oncotarget 8: 42510-42524, 2017.
38. Zhang X, Wen Z, Sun L, Wang J, Song M, Wang E and Mi X: TRAF2 regulates the cytoplasmic/nuclear distribution of TRAF4 and its biological function in breast cancer cells. Biochem Biophys Res Commun 436: 344-348, 2013.
39. Chung JY, Park YC, Ye H and Wu H: All TRAFs are not created equal: Common and distinct molecular mechanisms of TRAF-mediated signal transduction. J Cell Sci 115: 679-688, 2002.
40. Kedinger V and Rio MC: TRAF4, the unique family member. Adv Exp Med Biol 597: 60-71, 2007.
41. Camilleri-Broët S, Cremer I, Marmey B, Comperat E, Viguié F, Audouin J, Rio MC, Fridman WH, Sautès-Fridman C and Régnier CH: TRAF4 overexpression is a common characteristic of human carcinomas. Oncogene 26: 142-147, 2007.
42. Zhang X, Wen Z and Mi X: Expression and anti-apoptotic function of TRAF4 in human breast cancer MCF-7 cells. Oncol Lett 7: 411-414, 2014.